Development of a new bulk microphysical scheme for WRF with varying snow characteristics and riming intensity

Yanluan Lin and Brian A. Colle
School of Marine and Atmospheric Sciences, Stony Brook University, New York

1. Introduction

There are a wide variety of bulk microphysical parameterizations (BMPs) available in the Weather Research and Forecasting (WRF) model, ranging from the simple Kessler BMP to the latest Thompson scheme (Thompson et al. 2008). One of the critical parameters in a BMP is the treatment of snow and graupel. Most BMPs treat snow and graupel by assuming spherical particles with constant density. However, in reality, ice particles have a variety of habits and complex structures, while riming changes and modifies the properties of ice particles. Both ice habit and riming should be considered in BMPs to better represent the ice processes and precipitation fallout.

In general, there have been two approaches to include habits in BMPs. One is to increase the numbers of prognosed variables to simulate the different habits explicitly (Straka and Mansell 2005), while the other is to estimate the preferred habit at each grid point based on the local conditions (Meyers et al. 1997), which can be tracked by partitioning the snow category into different habit types (Woods et al. 2007).

Snow and graupel (or hail) are kept often as separate categories in traditional BMPs. Due to the large fall velocity difference between snow and graupel (or hail), the residence time and fallout of precipitation depends highly on the partition of snow and graupel, which has a large sensitivity on the surface precipitation distribution and precipitation efficiency (Lin and Colle 2008). By separately predicting the ice mixing ratios acquired through deposition versus riming, the riming effect on the mass and fall speed of snow can be considered (Stoelinga et al. 2007). Using a similar approach, Morrison and Grabowski (2008) considered the variation of particle properties with particle size and rimed mass fraction. Due to the size dependent properties, the method can be easily applied in a bin scheme. However, the approach has its shortcomings: only one habit type is used for nonspherical particles; it is difficult to derive a continuous mass-diameter (m-D) and area-diamater (A-D) relationships over the whole size spectrum; graupel size is smaller than partially-rimed particles; and analytical integration of total mass is impossible due to the size dependent m-D and velocity-diameter (V-D) relationships.

In this paper we propose a new bulk microphysical scheme for WRF (SUNY scheme), which relates the crystal habits and degree of riming directly to the ice properties (m-D, A-D, and V-D). By diagnosing a varying degree of riming, the continuous spectrum from pristine ice to slightly rimed ice to heavily rimed snow and graupel is represented.

**Corresponding author address:* Yanluan Lin, SoMAS, Stony Brook Univ. NY, 11794 email: yanlin@ic.sunysb.edu

2. Description of the new SUNY microphysical parameterization

The new scheme has four prognostic variables: nonprecipitating ice, precipitating ice (PI), cloud liquid water (CLW), and rain. Graupel is indirectly included in PI by the introduction of a degree of riming. The following focuses on the PI description of the BMP.

a. Ice crystal habits

Due to their irregular shapes, the geometry of ice particles is often described with a maximum diameter or dimension (called as D later). Power laws have been widely used to describe the m-D, A-D, and V-D relationships for ice particles:

$$m = a_m D^{b_m},\ A = a_a D^{b_a},\ \ V = a_v D^{b_v} \qquad (1)$$

Heymsfield et al. (2007) collected observations sampled from a wide range of temperatures to derive temperature-dependent coefficients (a_m and b_m) for the m-D relationship in Eq. 1 (see their Table 1). Using data collected in wave clouds, Baker and Lawson (2006) reported the A-D relationships for three crystal types (see their Table 4). These two studies provide the basis for the estimate of habit effect on m-D and A-D relationships in our BMP.

b. Riming intensity or degree of riming

Relatively few observations have been reported to describe the degree of riming (later referred to the riming intensity, Ri, which represents either partially-rimed particles or the rimed mass fraction of all particles). One approach is to define Ri as a function of the amount of CLW and PI in the scheme. For the preliminary tests, Ri is diagnosed as:

$$Ri = \sqrt{\frac{CLW}{PI}} \qquad (2)$$

and ranges from 0 (pristine ice particles) to 1 (graupel). More field observations, such as those collected in IMPROVE, will be utilized to further refine the Ri parameter in the future.

c. Mass-dimension and area-dimension relationships

In the m-D relationship, a_m can be considered as an effective density and b_m as a fractal dimension. Based on the “filling-in” concept proposed by Heymsfield (1982), the particle fractal dimension gradually increases with Ri and becomes 3 as the particle grows to a spherical graupel. Moismann et al. (1994, their Eq. 3) found that the rimed mass increased exponentially with Ri, which suggests a linear dependence of b_m on Ri. Moismann (1995, his Eq. 3) found that fall velocity of rimed particles increased as Ri^2. This suggests a linear increase of a_m with Ri^2 as illustrated in the derivation of V-D relationship later. More specifically, we propose the following, with the first two terms taken from Heymsfield et al. (2007) to reflect habit effect:

$$a_m = c_0 + c_1 T + c_2 Ri^2 \qquad (3)$$

$$b_m = C_0 + C_1 T + C_2 Ri \qquad (4)$$

We utilize the temperature dependent A-D relationship derived by Baker and Lawson (2006) and add the effect of Ri to get:

$$a_a = d_0 + d_1 T + d_2 Ri \qquad (5)$$

$$b_a = D_0 + D_1 T + D_2 Ri \qquad (6)$$

in which c_2, C_2, d_2, and D_2 are determined to bound the b_a and b_m by 2 and 3, respectively, and to ensure the new m-D and V-D relationship cover the wide range of variability observed.

d. V-D relationship

With the m-D and A-D relationships known, we follow the Best number (X) and Reynolds number (Re) approach to derive the V-D relationship (Mitchell 1996). This approach does not need an explicit drag coefficient and is relatively independent of the particle habit.

$$\mathrm{Re} = aX^b = \frac{DV}{\nu} \qquad (7)$$

$$X = \frac{2gmD^2}{\rho_a \nu^2 A} \qquad (8)$$

where g is the gravitational acceleration constant, ρ_a is the air density, and ν is the kinematic viscosity of the air. Incorporating (7) and (8) and using the m-D and A-D relationships defined in Eq. 3-6, we get

$$a_v = a\nu\left(\frac{2ga_m}{\rho_a \nu^2 a_a}\right)^b \qquad (10)$$

$$b_v = b(b_m - b_a + 2) - 1 \qquad (11)$$

From eq. (10), we see a_m needs to be proportional to Ri^2 to ensure the square dependence of V on Ri.

e. Ice capacitance

Particle capacitance is a function of the size and shape of the ice particle and it directly impacts the snow deposition and sublimation growth. Westbrook et al. (2008) showed that the capacitance of snow aggregates (b_m ~2) was only half that of a sphere. Since b_m linearly increases to 3 as Ri increases from 0 to 1, for simplicity, we assume (where C_s = 0.25 for dry snow):

$$C_s = 0.25(1 + Ri) \qquad (12)$$

3. Justification of the approach

This new ice parameterization has been implemented into WRF versions 2.2 and 3.0, with all the snow related processes in the scheme modified to use the newly derived m-D, A-D, and V-D relationships in equations 1-12. Since the spectrum of snow to graupel share the same category in this scheme, they also share the same processes. As compared with the traditional BMP with graupel, such as Thompson et al. (2008), the new scheme reduces the microphysical processes from over 40 to less than 20 (Fig. 1). This new scheme also saves the full run computation time by ~30%.

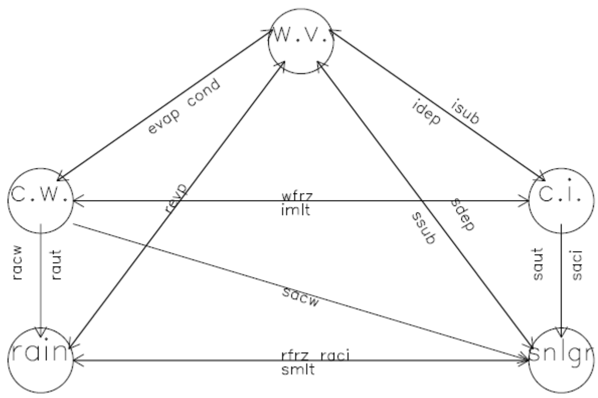

Figure 1. Microphysical flowchart for the new scheme. The circles represent the various water species (water vapor, cloud water, cloud ice, rain, PI), and the arrows are the processes that link them.

To illustrate the impact of Ri on m-D and V-D, Fig.2 shows the empirical m-D and V-D relationships for different habit types from Woods et al. (2007) and the m-D and V-D predicted in the SUNY scheme. As Ri increases from 0 to 1, the mass and fall velocity of PI increases accordingly and covers the wide range of observed m-D and V-D relationships.

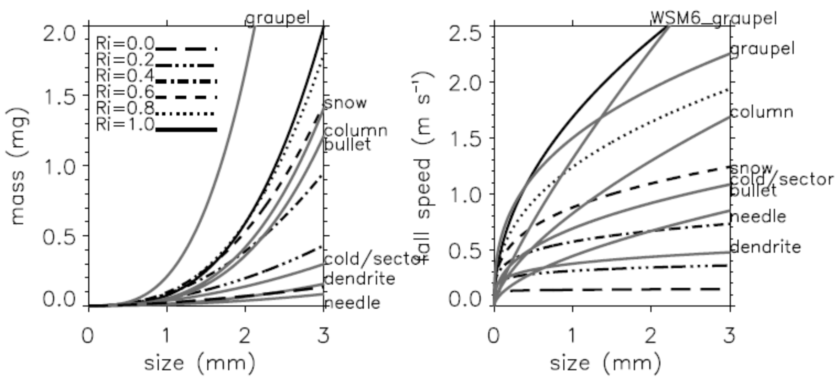

Figure 2. m-D and V-D relationships for snow and graupel used in traditional BMPs (denoted as snow and graupel) and for different types of ice particles (gray lines) from Woods et al. (2007). Also plotted are the temperature and Ri dependent m-D and V-D relationships used in the new scheme (black lines).

4. Preliminary tests

This new BMP was developed independent of IMPROVE microphysical field dataset, so we verify the approach against two IMPROVE-2 cases (13-14 and 4-5 Dec 2001). The model setup is identical to the settings used in Lin and Colle (2008). Here we focus on the precipitation and microphysics verification and comparison with the new Thompson scheme (Thompson et al. 2008) for the well-studied 13-14 December 2001 case.

The new SUNY produce two precipitation maxima over the coastal range and windward slopes of the Oregon Cascades (Fig. 3a). The SUNY scheme has ~20% more precipitation over the coastal range than the Thompson scheme (Fig. 3b), while SUNY reduces the precipitation over the windward slopes and crest of Oregon Cascades by ~20%. The new scheme verifies better with observations (Fig. 4), especially over the coastal range and Cascades windward slopes, but it has more precipitation into the lee than the Thompson scheme.

For the microphysics verification aloft (Fig. 5), the SUNY scheme has more CLW (~0.2 to 0.4 g m^{-3}) over the windward slopes of Cascades, which verifies better with observations (0.2 to 0.26 g m^{-3}). However, both the Thompson and SUNY scheme run underpredict the CLW over the lee by ~0.1 g m^{-3}. The SUNY scheme predicts maximum ice water content (IWC) of ~0.8 g m^{-3} just above the freezing level (~2 km MSL) compared with ~1.2 g m^{-3} by the Thompson scheme. As compared with the aircraft observations (Fig. 5), the new scheme reduces the IWC overprediction aloft by ~50%. Due to the underestimated CLW in the lee, the new scheme underpredicts the Ri and the fallout of the PI, which likely contributes to the larger spillover of snow into the lee.

Compared with observed RI (the ratio of graupel and total IWC), the new scheme predicts the observed RI within 0.2 with very light riming in the lee and large riming over the windward slopes (Fig. 6).

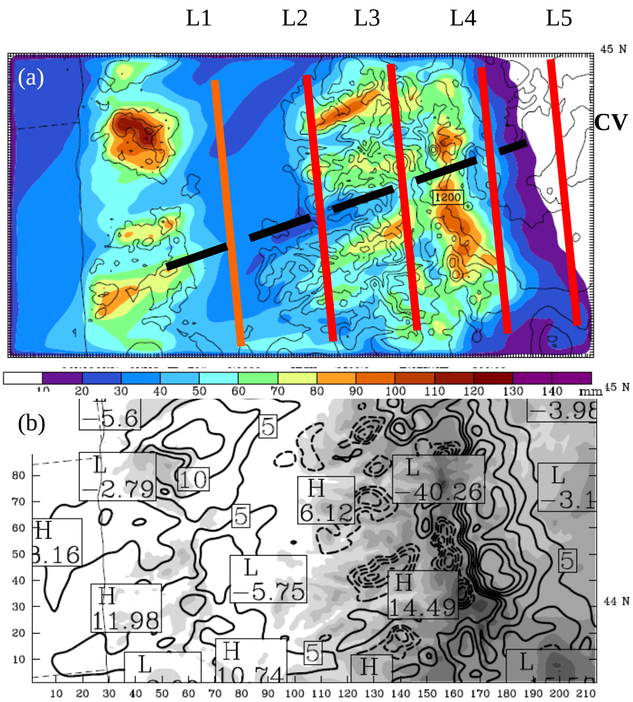

Figure 3. (a) SUNY 18-hour precipitation (color shaded every 10 mm) for the 1.33-km WRF domain between 1400 UTC 13 Dec and 0800 UTC 14 Dec 2001 and 1.33-km terrain is contoured for reference. The lines denote the P3 (red lines) and Convair flight legs (black dashed lines). (b) the precipitation difference (in mm) between the SUNY and Thompson runs.

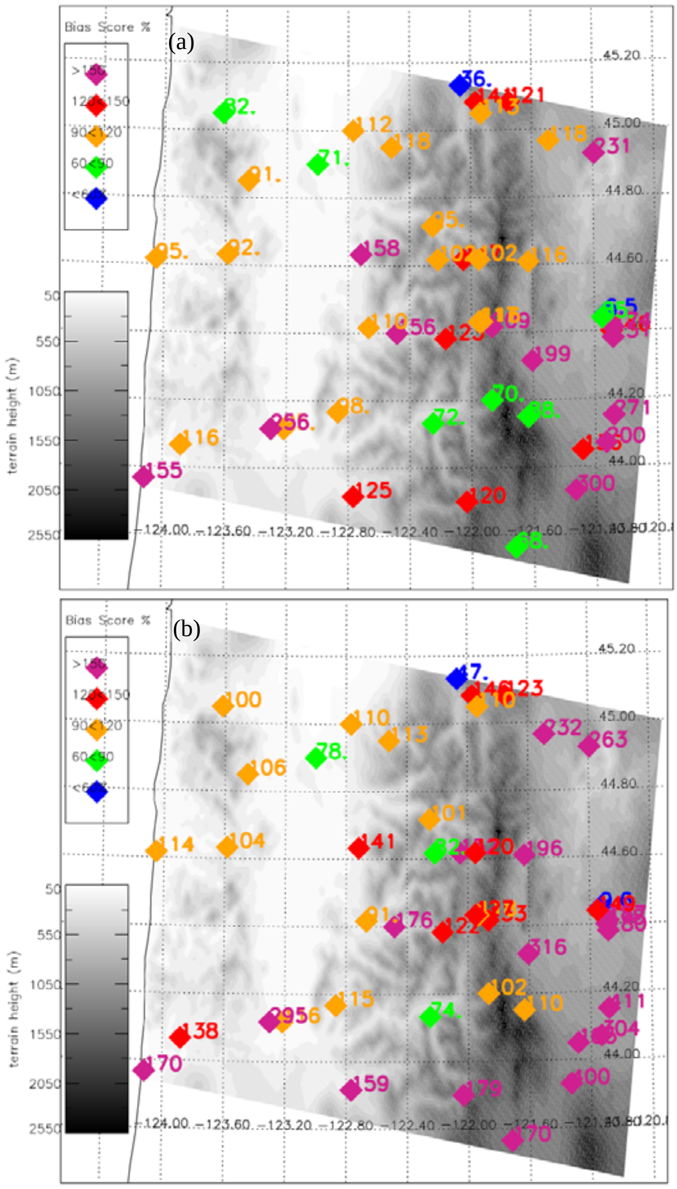

Figure 4. 18-h WRF percent of observed precipitation between 1400 UTC 13 Dec and 0800 UTC 14 Dec 2001 for the (a) Thompson and (b) SUNY schemes.

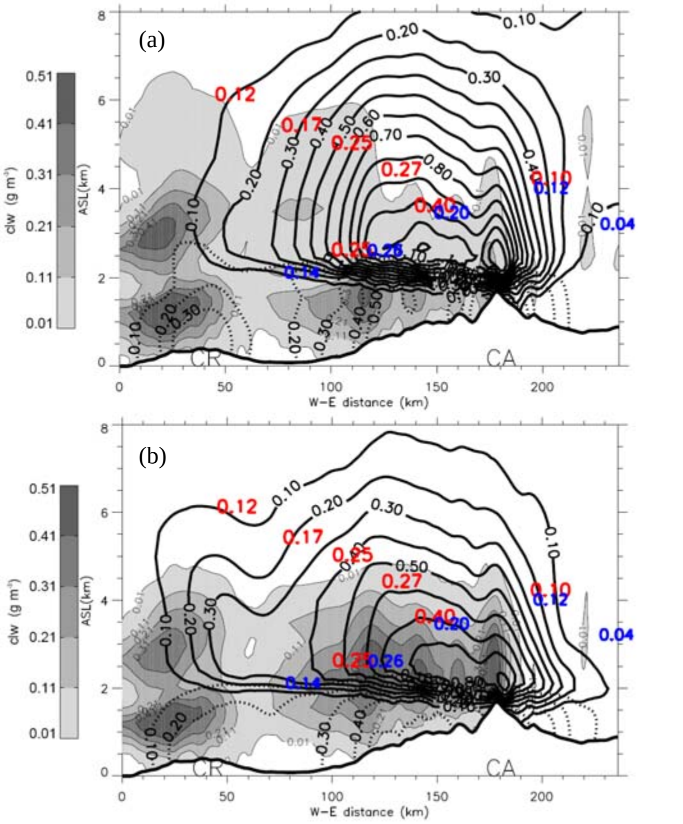

Figure 5. 2-h mean (between 2300 and 0100 UTC 13-14 Dec) east-west cross section showing the IWC (solid lines, every 0.1 g m^{-3}), CLW (shaded), and rain (dotted lines, every 0.1 g m^{-3}) for (a) Thompson and (b) SUNY scheme. Overlaid are leg-mean IWC (red) and CLW (blue) measured by Convair and P3.

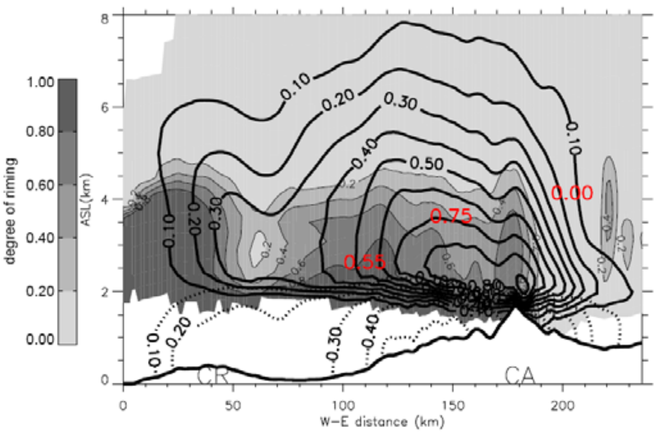

Figure 6. Same as Fig. 5, except showing the riming intensity (shaded) of the new scheme. Overlaid red numbers are the riming intensity measured by P3.

5. Conclusions

Preliminary tests of the new SUNY scheme suggest the proposed approach using a riming intensity (Ri) and continuous snow to graupel category is promising. Future work will use more observations to better quantify Ri, include hail, and double moment characteristics.

6. Acknowledgements

This work was supported by the National Science Foundation (ATM-0450444).

7. References

Baker B., and R. P. Lawson, 2006: Improvement in determination of ice water content from two-dimensional particle imagery. Part I: Image-to-mass relationships. *J. Appl. Meteor. Climatol.*, **45**, 1282–1290.

Heymsfield A. J., 1982: A comparative study of the rates of development of potential graupel and hail embryos in high plains storms. *J. Atmos. Sci.*, **39**, 2867–2897.

Heymsfield A. J., G.-J. van Zadelhoff, D. P. Donovan, F. Fabry, R. J. Hogan, and A. J. Illingworth, 2007: Refinements to ice particle mass dimensional and terminal velocity relationships for ice clouds. Part II: Evaluation and parameterizations of ensemble ice particle sedimentation velocities. *J. Atmos. Sci.*, **64**, 1068–1088.

Lin, Y., and B.A. Colle, 2008: The 4-5 December 2001 IMPROVE-2 event: Observed microphysics and comparison with the WRF model. Submitted to *Mon. Wea. Rev*.

Meyers, M.P., R.L. Walker, J.Y. Harrington, and W.R. Cotton, 1997: New RAMS cloud microphysics parameterization. Part II: The two-moment scheme. *Atmos. Res.*, **45**, 3-39.

Mitchell D. L., 1996: Use of mass- and area-dimensional power laws for determining precipitation particle terminal velocities. *J. Atmos. Sci.*, **53**, 1710–1723.

Mosimann L., E. Weingartner, and A. Waldvogel, 1994: An analysis of accreted drop sizes and mass on rimed snow crystals. *J. Atmos. Sci.*, **51**, 1548–1558.

Moismann L., 1995: An improved method for determining the degree of snow crystal riming by vertical Doppler radar. *Atmos. Res.*, **37**, 305-323.

Morrison H., and W.W. Grabowski, 2008: A novel approach for representing ice microphysics in models: description and tests using a kinematic framework. *J. Atmos. Sci.* In press.

Stoelinga M, H. McCormick, and J. D. Locatelli, 2007: Prediction of degree of riming within a bulk microphysical scheme. Presented on 22nd Conference on Weather Analysis and Forecasting/18th Conference on Numerical Weather Prediction.

Thompson, G., P.R. Field, R. M. Rasmussen, and W.D. Hall, 2008: Explicit forecasts of winter precipitation using an improved bulk microphysics scheme. Part II: Implementation of a new snow parameterization. *Mon. Wea. Rev*. In press

Westbrook C. D., R. J. Hogan, and A. J. Illingworth, 2008: The capacitance of pristine ice crystals and aggregate snowflakes. *J. Atmos. Sci.*, **65**, 206–219.

Woods C. P., M. T. Stoelinga, J. D. Locatelli, and P. V. Hobbs, 2007: The IMPROVE-1 storm of 1–2 February 2001. Part III: Sensitivity of a mesoscale model simulation to the representation of snow particle types and testing of a bulk microphysical scheme with snow habit prediction. *J. Atmos. Sci.*, **64**, 3927–3948.